

Space-based Sensors for Extreme Fire Weather Events

Aaron Pereira^{a,d}, Jason Sharples^b, Fred Menk^c, Ed Kruzins^b, Roger Kermode^a, Said Al-Sarawi^d, Derek Abbott^d, Caroline Polusen^e, Murzy Jhavbala^f, Doug Morton^f, Patrick Gatlin^g, Mason Quick^g, and Paulo de Souza^h

^aUniversity of Technology, Sydney, Australia

^bUNSW Canberra, Canberra, ACT, Australia

^cUniversity of Newcastle, Newcastle, NSW, Australia

^dUniversity of Adelaide, North Terrace, SA, Australia

^eBureau of Meteorology, Melbourne, VIC, Australia

^fNASA Goddard Space Flight Center, Greenbelt, Maryland, USA

^gNASA Marshall Space Flight Center, Huntsville, Alabama, USA

^hEdith Cowan University, Joondalup, WA, Australia

ABSTRACT

Catastrophic bushfires are becoming increasingly prevalent as climate change advances. Impacts extend beyond national borders. Multinational efforts can inform new science and management practices. Space-based sensors and integrated data facilities will play an important role. This paper describes a collaborative project between a consortium of Australian universities and NASA Centers to develop and implement a small satellite platform comprising highly integrated thermal and lightning sensors coupled with AI-based edge computing to help predict, detect, and track bushfires, supporting mitigation activities. This will fill an important capability gap since Australia does not currently have any sovereign Earth observation satellites. This program is enabled by and builds on Australia-NASA collaboration and will also support fire science and management activities in the broader global context.

Keywords: Space Sensors, Bushfires, Lightning Detectors, Thermal Imagers

1. INTRODUCTION

Australia is the driest inhabited continent on Earth. It is also one of the planet's most diverse countries, with half the world's marsupial species, and where 85% of plant species are unique. It is estimated that 70% of all Australian species of plants, animals, fungi and other organisms are yet to be discovered and documented.¹

Australia experiences some of the world's most extreme bushfires. Fires in 2019-20, mostly triggered by lightning following extreme drought conditions, destroyed an area the size of the United Kingdom including over 3,000 buildings, the world heritage Gondwana rainforests, and killed or displaced nearly 3 billion animals.² Smoke exposure led to a 6% increase in respiratory disease admissions and a 10% increase in cardiovascular disease.³ Particulate emissions circulated around the globe, cooling the southern Pacific and possibly triggering the 3-year La Niña climate cycle.⁴ Such events will become more likely and intense under climate change.⁵ With Australia's large land mass and distributed population centres, Earth orbiting satellites are ideal platforms to support environmental and fire management. Australia has no such sovereign capability.

Here we detail a program to advance fire science and management by developing, launching and operating a small Australian satellite to support bushfire management including fuel load monitoring, lightning flash detection, situational awareness, air quality assessment, post-fire recovery, and fire science activities. The project

Further author information:

Aaron Pereira: E-mail: aaron.pereira@uts.edu.au, Telephone: +61 3 83134198

Jason Sharples: E-mail: j.sharples@unsw.edu.au, Telephone: +61 2 5114 5020

leverages state-of-the-art thermal imaging and lightning detection sensors developed by the National Aeronautics and Space Administration (NASA) Goddard (GSFC) and Marshall Space Flight Centers (MSFC), integrated with on-board artificial intelligence (AI) computing and using facilities and capabilities across an Australian consortium of universities, the Bureau of Meteorology, and industry partners. Observations will focus on detections during the late afternoon when fires are at their peak.

The project will also support national environmental and agricultural management and weather forecasting by monitoring ground and sea surface temperatures, and help monitor fire activity across Asia-Pacific, the Amazon region, and tropical Africa. A collateral mentoring and training program and STEM engagement program with schools will support national workforce development.

The bushfire satellite will form a pathfinder for further Australian small satellites with a greater range of capabilities, increasing sovereign space capability and contributing to national and multinational environmental science and management programs, including where appropriate, complementary operation and reciprocal data exchange with international partners. This project results from and advances strategic mission-based collaboration between Australia and NASA. This is a unique partnership enabling Australia to leverage hard-won expertise and IP from NASA for national benefit and national and societal benefit. The intention is to grow Australian capability and capacity to support more complex multinational space programs.

This paper is organized as follows. This Introduction has summarized the growing significance of extreme bushfires in Australia and the consequent requirement for space-based sensors. Section 2 outlines key aspects concerning the dynamics and space-based monitoring of extreme bushfires in Australia. The role of lightning in triggering such fires, and requirements for satellite-based lightning detection, are discussed in Section 3. Section 4 describes the stepwise approach to developing a small satellite program meeting these objectives. Details of the sensor payloads are provided in Section 5, while Section 6 describes the satellite platform and ground segment. The paper concludes with acknowledgments and references.

2. BUSHFIRES IN AUSTRALIA

Australia has a long history of destructive bushfires, with the most significant impacts occurring in the more densely populated, and more heavily forested, southern parts of the continent. However, climatic changes driven by anthropogenic emissions are producing longer fire seasons with conditions more conducive to large and destructive bushfires.^{6,7} These changes have been associated with a multidecadal increase in annual area burned in Australia⁵ and an increase in the prevalence of extreme bushfires.^{8,9}

Extreme bushfires are initiated via dynamic escalation in fire behavior and intensity and driven through significant coupling between a fire and the surrounding atmosphere. This modifies or maintains the fire's propagation through processes such as strong pyrogenic winds and mass spotting, which can lead to the formation of zones of intense and widespread flaming. The large spatial integral of instantaneous energy release associated with widespread flaming reinforces the vigor of the plume, which maintains the strong coupling of the fire with the atmosphere. Extreme bushfires often manifest as towering pyrocumulus (pyroCu) or pyrocumulonimbus (pyroCb) storms, but can also cause extensive damage as wind-driven violent pyroconvective events.

PyroCb have been associated with some of Australia's deadliest and most destructive fire-related catastrophes, including Ash Wednesday in 1983, Black Saturday in 2009 and most recently during the 2019-20 Black Summer. They have become increasingly common across southern Australia – of all the pyroCb events currently recorded in the Australian PyroCb Register,¹⁰ which dates back to the start of the satellite record, 94% have occurred since 2003, while 33% were recorded during the 2019-20 Black Summer fire season alone.

Monitoring fire activity and identifying pyroCb occurrence across the vast expanse of the Australian continent is a challenging exercise that is greatly assisted by the availability of space-based sensors. A key diagnostic of pyroCb activity is the presence of ice in large anvil clouds in the upper troposphere and/or lower stratosphere. As such, pyroCb activity can be detected using thermal infrared (11 μm) cloud-top brightness temperature imagery from the Advanced Himawari Imager (part of the Himawari 8/9 satellite payload). Specifically, pyroCb detection relies on the presence of 11 μm brightness temperatures lower than the homogeneous liquid water freezing threshold of -35°C , which is incorporated as part of a bespoke pyroCb detection algorithm.^{11,12}

The initial escalation of extreme bushfires typically results from dynamic fire behaviors, which are driven by interactions between winds, fuels, certain topographic features and the fire itself.^{8,13} However, research into dynamic fire propagation is still a burgeoning area of inquiry. Improvements in our ability to predict, or even anticipate, instances of dynamic fire behavior are currently limited by access to suitable data to support model development and evaluation. Space-based sensors can play a central role in the provision of such data, provided they capture fire activity at appropriate spatiotemporal scales.

Currently, the sensors on Himawari 9 provide data at temporal resolutions of 10 minutes (or less) but only at spatial resolutions of several hundred meters or more. Other sensors that provide higher resolution spatial data do not have the temporal resolution to permit tracking of fire dynamics over sub-hourly time scales. Ideally, information that captures fire progression at spatial scales of around 50 m and at a temporal resolution of around 30 minutes would be required to support the development and evaluation of next-generation fire propagation models that are able to accurately capture dynamic behaviors and the associated escalation of fire complexes. Indeed, a suitable suite of space-based sensors that captures fire progression data over the southern expanse of Australia would facilitate the development of advanced fire propagation models incorporating the latest knowledge of bushfire dynamics and data-driven modelling approaches.

Space-based sensors also have critical roles to play in other aspects of bushfire detection and monitoring. For example, monitoring hotspots (or the absence of such) is critical to the detection and tracking of the growth of bushfires, and key in the diagnosis of blow-up fire events and extreme bushfire development. Satellite-based sensors also play a key role in monitoring smoke and other emissions from bushfires, including stratospheric aerosol injections that have important ramifications for global climate.^{7,12} Space-based sensors also provide information that is needed to assess bushfire potential and as inputs to bushfire spread models. This includes information on landscape dryness, landscape attributes, fuel load and moisture content and vegetation type and cover. Lightning detection remains a key application of space-based sensors. Indeed, analysis of lightning data in conjunction with other environmental factors is currently an area of intense research interest, which is providing deeper insights into the ignition of bushfires by lightning and how these occurrences interact with critical fire weather events driven by synoptic-scale circulations.¹⁴

3. BUSHFIRES AND LIGHTNING

Bushfires can originate from both human activity and natural causes with lightning the predominant natural source. This accounts for about half of all ignitions in Australia and most of the damage including about 80-90% of the area burnt in the case of the black summer fires in 2019-20. This is because of the difficulty in identifying fires early in remote locations and mobilizing resources. While some variables such as fuel flammability are possible to predict days to weeks in advance, lightning is difficult to predict.¹⁵

Lightning is one of the most spectacular and hazardous phenomena on the planet. It is responsible for many fatalities and significant damage worldwide.¹⁶ Its intimate link to extreme weather and influence on major greenhouse gases has motivated its listing by the World Meteorological Organization as an essential climate variable. Amongst the impacts attributed to lightning strikes are bushfires. Positive cloud-to-ground lightning strikes (+CG) and their tendency to produce long continuing current have long been the focus of lightning-ignited bushfire studies.^{17,18} A recent study comparing 26-years of bushfires and CG strikes found no +CGs within 10 km of 62% of the lightning-ignited bushfires in the contiguous U.S and attributed over 90% of the ignitions to negative CGs.¹⁹ Since the number and impact of lightning-ignited bushfires is projected to increase over the coming decades,^{20,21} it is imperative that we gain a better understanding of the electrical characteristics of thunderstorms that produce these types of lightning so that we might be able to better detect them in the future.

Lightning-ignited fires can begin in grassland but are typically initiated in forested areas. Trees can often be destroyed by lightning strikes. When lightning hits a tree, it usually travels just below the tree's bark where there is a layer of sap and water. This layer becomes instantly heated and expands causing the bark to be blasted off the tree and sometimes splitting the wood. While the fire is often instantaneous it can smoulder within a tree and not begin to spread until several days later.²²

The Final Report of the NSW Bushfire Inquiry 2020²³ noted of the fires “many of which were started by lightning in remote or rugged terrain and quickly got to the point where suppression of the fires was extremely difficult. The dryness of the landscape due to prolonged and widespread drought meant that lightning ‘caught’ well to start fires and provided suitable conditions for them to spread once they were alight”.

Identifying a fire early is key to prioritizing fire resources and decreasing the response time to tackle the fire. The Bureau currently monitors lightning using a network of ground sensors provided by Weather Zone in partnership with Earth Networks, as shown in Figure 1.²⁴ Ground-based lightning location systems detect Radio-Frequency (RF) signals produced by lightning. In addition to the time and location, the low and high-frequency networks (< 300 MHz) can discern the polarity of the strike and estimate its peak current. These primarily detect CG flashes, but some stronger cloud flashes can also be detected. Very high frequency (VHF) networks are used to detect cloud flashes, which comprise the vast majority of lightning activity in a thunderstorm, and map those with high accuracy in three dimensions (3-D) within 100 km of the network center.²⁵ Additionally, the electrical charge structure of thunderstorms can be inferred from these VHF measurements.²⁶

Satellite-based lightning mappers detect both CGs and intracloud flashes but cannot discern between the two. They measure the optical attributes of lightning and can be used to train models that detect continuing current flashes with high success rates.²⁷ Since 2016, the Geostationary Lightning Mapper (GLM) onboard the GOES-R satellites provide total lightning coverage over the Americas.²⁸ The Meteosat Third Generation Lightning Imager (MTG-LI) detects total lightning activity over Europe and Africa.²⁹ Another operational lightning mapping instrument onboard the Chinese Fengyun-4A geostationary satellite provides seasonal coverage over China and a portion of western Australia.³⁰

What is needed is a dedicated effort to document both the RF and optical characteristics of lightning and thunderstorms that ignite bushfires. This would entail deploying both a VHF network like the Lightning Mapping Array (LMA) to observe the 3-D electrical structure of thunderstorms along with lower frequency electric field change meters to estimate the current and polarity of CG flashes in a bushfire-prone region.^{31,32} Additionally, coincident optical measurements could be made from a ground-based or preferably airborne platform

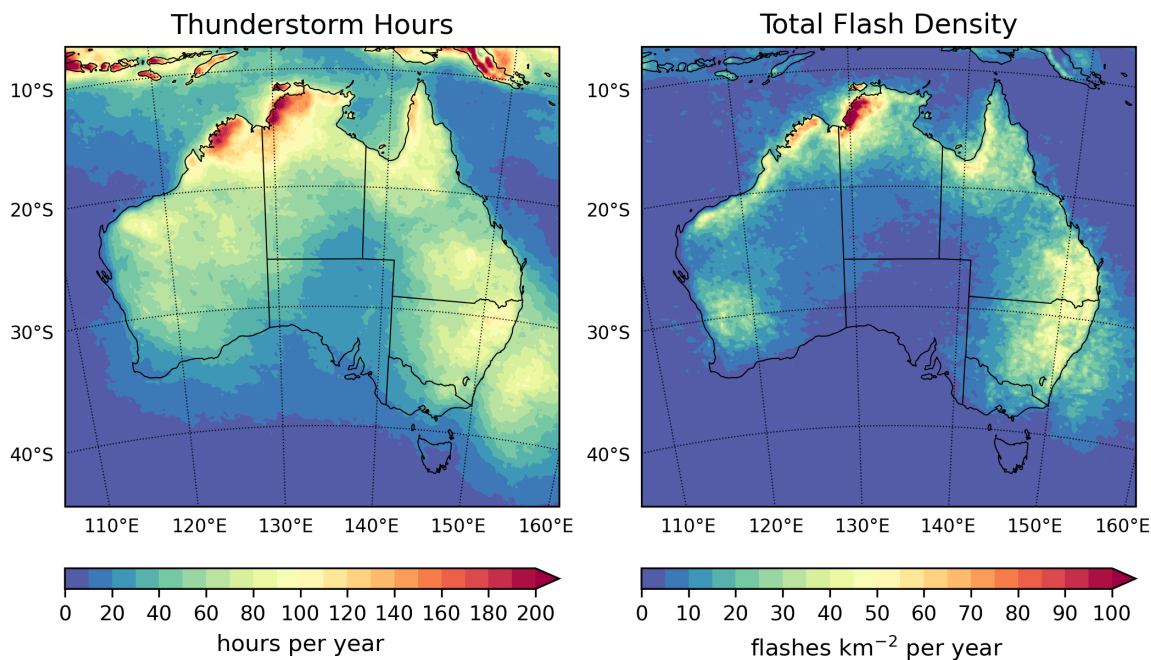


Figure 1. Mean annual number of thunderstorm hours (defined as two or more lightning strokes recorded in a 20 km × 20 km grid cell) and the corresponding annual average lightning stroke density detected by WZTLN.

to observe the radiometric attributes of these flashes. Future lightning mapping instruments are being developed and satellite-based missions formulated at NASA MSFC to utilize the strengths of both VHF and optical measurements of lightning.^{33,34} Combined, these observations can inform the development of a satellite-based capability to detect lightning-ignited bushfires on a global scale.

4. PATH TO FLIGHT

The path to flight consists of a stepwise approach to minimize the risk while achieving the program objectives. Figure 2 shows the evolution to an airborne mission then toward an orbital mission. This approach involves development and deployment of ground based lightning detectors to provide high fidelity ground truth observations and characterization of flashes that initiate fires. The airborne campaign would follow to measure the optical characteristics of fire initiators to inform orbital mission requirements. A necessary step is testing on high altitude platform (e.g. ER-2) to confirm functionality before being integrated together with a compact thermal imager onto to a small form factor platform (e.g. CubeSat) for an orbital mission.

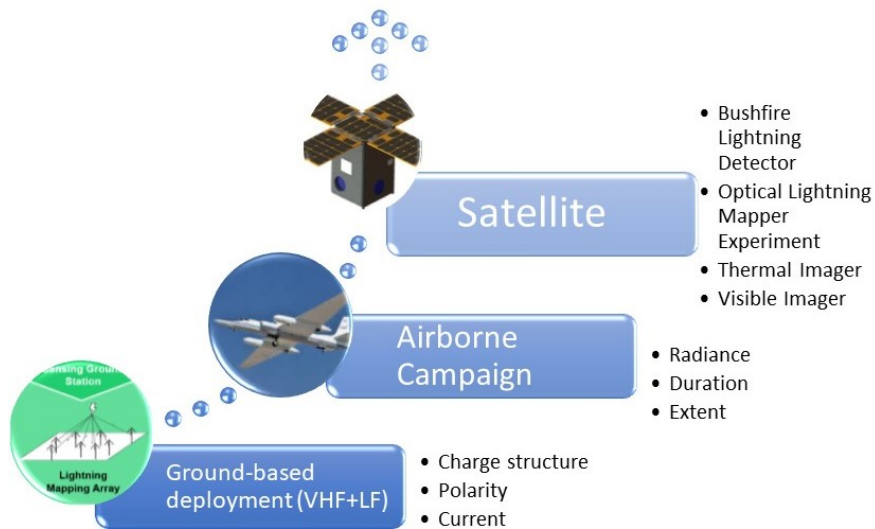


Figure 2. A calibrated approach to mitigating the risks associated with the mission is adopted. This includes airborne campaign to calibrate and validate the sensor suite. The next phase is the orbital campaign currently based-lined for a 12U CubeSat.

The major steps for the path to flight include:

- Finalizing the Detailed Scientific Matrix: Thermal and lightning parameters for bushfire ignition, triage, and behaviour versus fuel loading, type, terrain, and weather.
- Confirming Technical Feasibility: Evaluate if the current thermal and lightning sensors and supporting technology can be adapted for airborne flight rather than a space mission. This includes assessing mass, power, data transmission, and environmental factors.
- Ensuring Airborne and Space Mission Objectives: Align the airborne campaign with the science matrix and assess the airborne mission’s goals, sensors, data collection methods, and operational procedures to meet the science matrix requirements. If successful, adapt with a view toward a space mission.
- Integrate Sensor and Payload Development: Thermal sensor test and evaluation to meet science objectives and consistency with airborne integration. Lightning sensor test and evaluation to meet science objectives and consistency with distributed ground placements in target locations. Adapt the flight model to a small form factor space mission.

- **Prototype Testing:** Create and test prototypes to ensure all systems function correctly initially in the airborne and then space environment.
- **Adaptation of Sensors:** Modify or redesign sensors for flight conditions. This includes addressing accommodation constraints and vibration considerations for the airborne mission but then redefining for a launch and space environment.
- **Adapt from the Airborne to the Space Frame:** Design and build the thermal payload for airborne flight, which will include the adapted sensors and any additional equipment required for operation. Redesign and rebuild both thermal and lightning payloads for space.
- **Calibration and Validation (Cal/Val):** Establish thermal and lightning Cal/Val sites and conduct calibration of airborne instrumentation to ensure accurate data collection.
- **Endorse a Concept of Operations (CONOPS) and logistics:** Establish and optimize target locations, area and flight paths consistent to meet mission and science objectives. Establish flight certifications, licensing and consistency with regulations. With a successful airborne Cal/Val of target sites, rework the CONOP for a space mission.
- **Plan for Contingencies:** Establish backup options to mitigate the airborne campaign risk and with its success prepare contingencies for integration, launch and operations for a space mission.

Mitigating the risks associated with the mission guides us to an airborne campaign to Cal/Val the sensor suite and adds confidence to attempt the next phase which is an orbital campaign currently baselined for a 12U CubeSat.

5. SENSOR DETAILS

5.1 Multispectral Compact Thermal Imager

The Multispectral Compact Thermal Imager (MCTI) is a fully portable, 6-band multispectral camera that was conceived, designed and manufactured to be a ground-based instrument to complement the thermal instrument on the future Landsat-Next mission. It is an evolutionary advancement over a previous dual-band IR imaging instrument NASA GSFC had developed and installed on the International Space Station (ISS) in 2018.^{35,36}

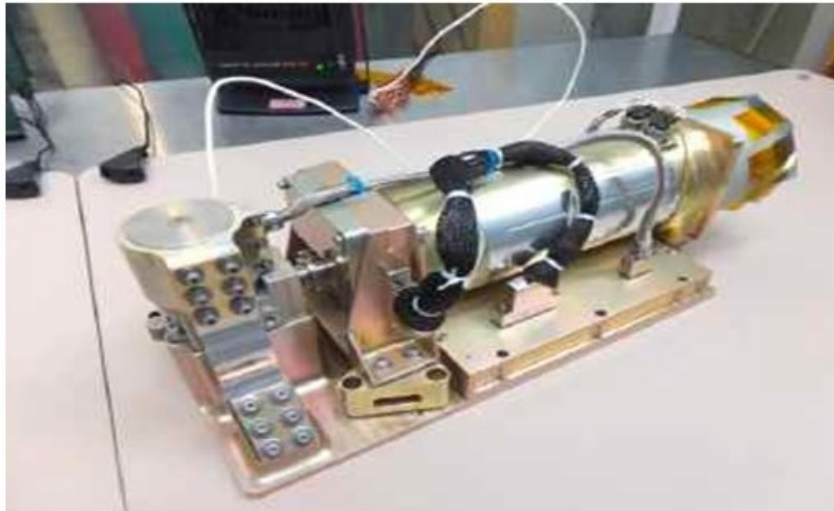


Figure 3. The Compact Thermal Imager flown on the International Space Station in 2018-2019.

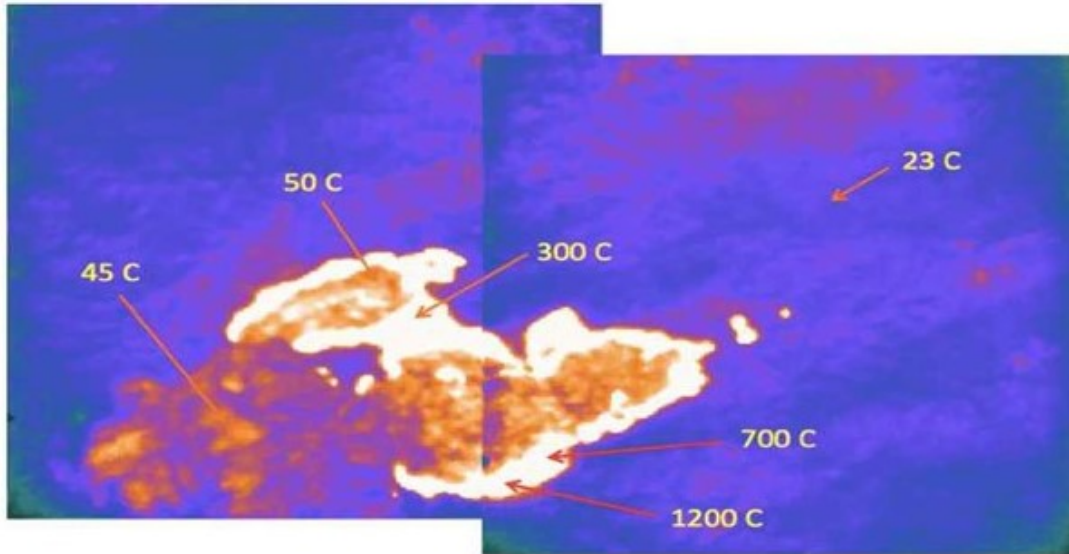


Figure 4. Fire in eastern Australia observed by CTI on November 8, 2019. Highest temperatures are on the fire fronts. Previously burned areas behind the fronts are cooler, but still warmer than the unburned area at upper right.

This original Compact Thermal Imager (CTI) acquired over 15 million images during its mission lifetime including many over large parts of the earth during the severe 2019 fire season. Figure 3 show CTI Flight instrument. An image of Australia captured during the bushfire season of 2019-20 is shown in Figure 4. Another image dataset obtained for the coastline of UAE is shown in Figure 5.

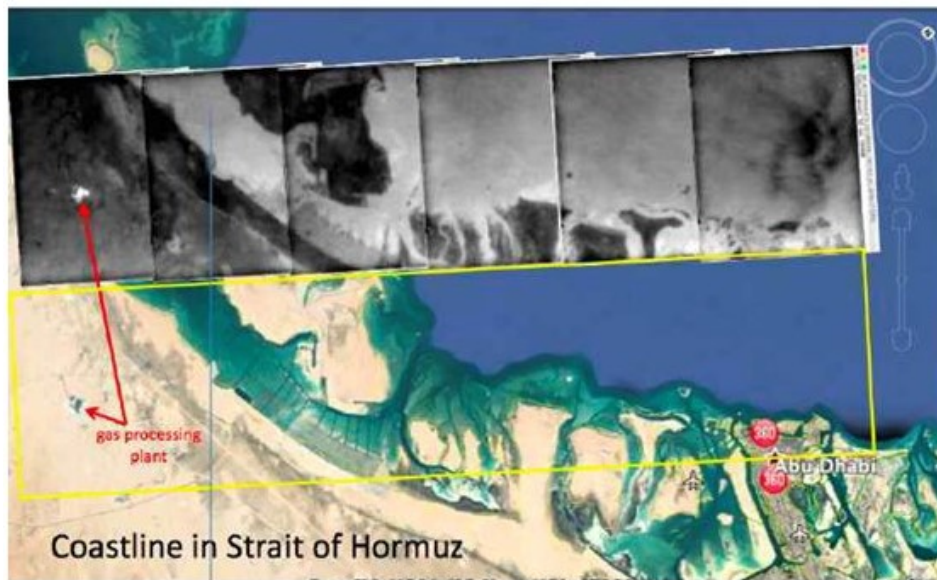


Figure 5. CTI image of shoreline near Abu Dhabi, United Arab Emirates, compared with Google Earth. Yellow rectangle shows the area of overlap. The hot burn-off plume from a gas refinery is easily identified. Variations in infrared brightness of the water surface because of temperature and emissivity of effluents from estuaries.

A photograph of the next generation Multispectral Compact Thermal Imager is shown in Figure 6 . The goal was to specifically design and build a fully portable, 6 band infrared camera covering the 3-12 μm IR spectrum. The camera is based on the Strain Layer Superlattice (SLS) infrared detectors being fabricated in the Goddard

Detector Development Laboratory (DDL). Additionally, the recently developed DDL process of attaching filter elements directly to the detector surface will be implemented to further demonstrate the advancement of GSFC in-house focal plane fabrication capabilities.

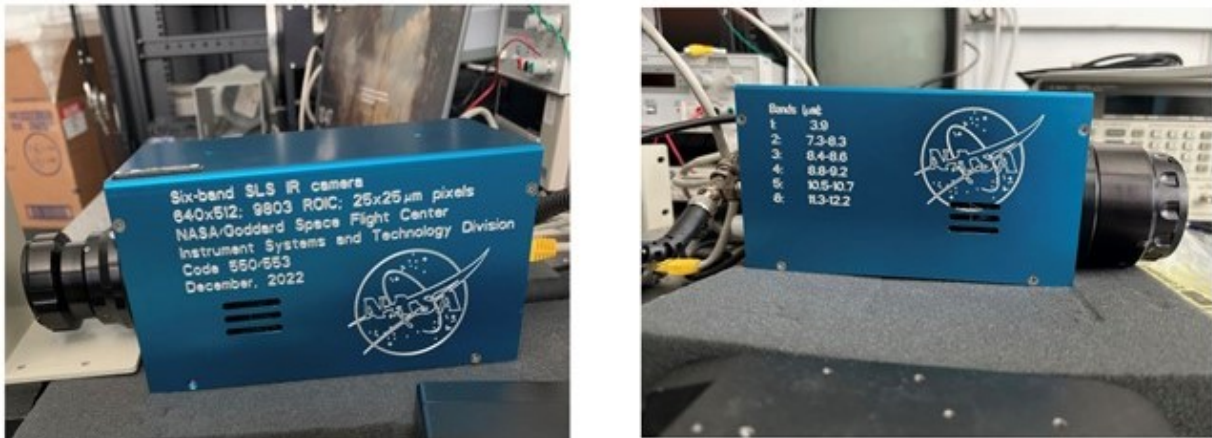


Figure 6. Photographs of the MCTI camera with a 25 mm (left) and a 50 mm (right) lens attached. The camera housing is 7" × 4" × 4" (18 × 11 × 11 cm). The lens mount is a standard bayonet mount which allows for lenses to be easily changed depending on the application.

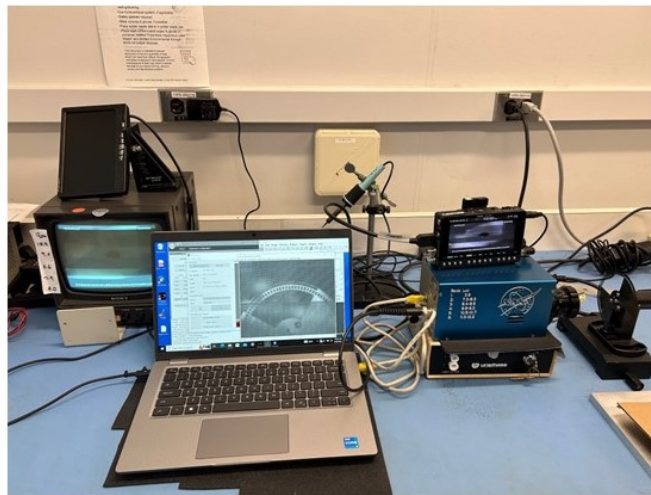


Figure 7. The MCTI camera system. A laptop monitors and stores the data. The PIX-E5 shown sitting on top of the camera records live video. Displayed is an image of the chopper wheel. Other video recorders are commercially available. The PIX-E5 will store the video for any data analysis at a later date.

The camera is powered by a 24 V DC power adapter and is controlled by a laptop with custom camera software shown in Figure 7. The laptop displays and stores the images, but post-data acquisition processing is necessary to optimize the data reconstruction and display the entire image in each band. A 30 Hz video port allows for real-time video display and storage which is particularly useful during the actual flights. A variety of video devices can be used for this purpose. The small PIX-E5 module shown on top of the camera provides optimal solution for the current requirement. This video unit has been trialed on previous IR imaging flights. Each frame is 5.3 Mbits (16 bits/frame times 512 x 640) at 60 frames per second (fps) and this generates a significant amount of data. (2 Gbytes/min).

Figure 8 shows the MCTI imager attached to a Goddard airborne platform, the complete camera system



Figure 8. MCTI camera mounted on a Goddard airborne platform (G-LiHT).

including laptop and PIX-E5 and recent photograph of the MCTI installed on the GLiHT instrument ready for airborne flights over southern Virginia is given in Figure 9. In this configuration, two connections are required: a power cable and a cable from the camera to a laptop. The laptop is manned during these flights. External hard drives can be switched in and out of the laptop depending on the data storage requirements.



Figure 9. The MCTI camera installed on GLiHT for flights over southern Virginia in July 9-16, 2024.

The testing/screening program includes measuring the:

- Dark Current vs. Bias Voltage and Temperature
- Relative Spectral Response/Absolute Quantum Efficiency
- Noise Performance
- Nonfunctional Pixels
- Survival of Power Cycle
- Power Dissipation

The detector performance parameters are listed in Table 1. The absolute quantum efficiency in each spectral band is shown in Figure 10. This plot convolves the unfiltered spectral response with the measured transmission of each filter segment. Each filter band response was measured from 3-25 μm .

Table 1. Detector Hybrid and System Parameters.

Parameter	Value
Array Format	640 × 512 cm
Pixel Pitch	25 μm
ROIC	ISC9803
Frame Rate	60 fps (max)
Camera Lens	25 mm
Operating Temperature	70-75 K
Band 1 Band Pass	3.95-4.05 μm
Band 2 Band Pass	7.3-8.3 μm
Band 3 Band Pass	8.4-8.6 μm
Band 4 Band Pass	8.8-9.2 μm
Band 5 Band Pass	10.5-10.7 μm
Band 6 Band Pass	11.3-12.2 μm
Filter Band Format	640 × 85 pixels/band
Dead Pixels	1039 (99.68% yield)
Dark Current	$(0.8 - 2.6) \times 10^9$ e/s-pix
Average Quantum Efficiency (QE) 3.5-11.5 μm with filters	15-30%
Total Noise	600 e^-
Detector hybrid power dissipation	145 mW
Total System Power	75 W
Camera Weight (excluding laptop)	4 kg

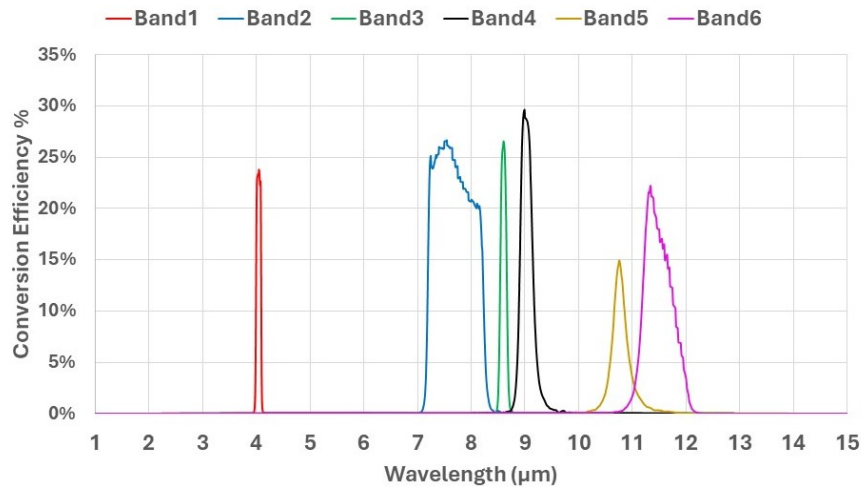


Figure 10. Spectral quantum efficiency of the detector hybrid with filters attached.

5.2 Lightning Detector

During the airborne campaign, a ground-based system of lightning detectors will be deployed in a region of South Eastern Australia frequented by lightning-ignited bushfires. This will include NASA's deployable LMA network,³¹ which consists of 10-12 VHF stations (Figure 11), to locate the pathways of lightning channels and map out the electrical charge regions within the cloud. These observations will be highly complementary to the long-range lightning location system currently used by Australia's Bureau of Meteorology and combined will provide a complete picture of the origin, type, and peak current of flashes that contact the ground in a fire-prone region.



Figure 11. An example of a deployable LMA receiving station that is used along with other LMA stations to map the 4-D structure of lightning within a thunderstorm.

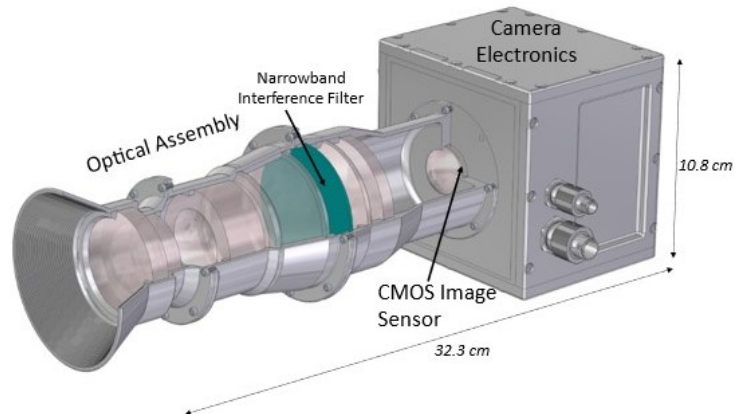


Figure 12. A compact lightning mapper being designed to measure the radiant energy of optical pulses associated with ground and cloud flashes.

In a subsequent airborne campaign, a high-altitude aircraft (e.g., ER-2) will be used to fly a prototype of the CubeSat Lightning Detection Experiment (CLIDE) over the tops of thunderclouds, including pyro-cumulonimbus,

to document the optical characteristics of lightning that ignites bushfires as it would be seen from a space-based optical lightning mapper. CLIDE is a new lightning mapper concept to improve detection of smaller and more optically dim pulses from lightning.³⁴ It consists of two CMOS image sensors to measure the cloud-top emissions in the near-infrared (777.4 nm) and ultraviolet (337 nm) from hot and cold lightning processes. The prototype shown in Figure 12 is for a version of CLIDE that will be flown on the airborne campaign—two of these barrel-type imaging systems will be used for each channel.

A more compact imaging system with folded optics is envisioned for the spacecraft version. By using a CMOS image sensor combined with a Xilinx FPGA the size, weight, and power of the camera electronics are significantly reduced compared to heritage LEO lightning mappers.³⁷ The Flys-Eye GLM simulator, which is an array of optical radiometers designed for measuring cloud-top optical emissions from lightning,³⁸ may also be flown on the high-altitude aircraft to better resolve the spectral characteristics of cloud-top emissions from lightning that ignites bushfires. Combined with observations from the ground-based VHF and LF networks, these airborne observations will be critical in developing a space-based capability to detect naturally occurring bushfire ignitions.

5.3 Edge Computing

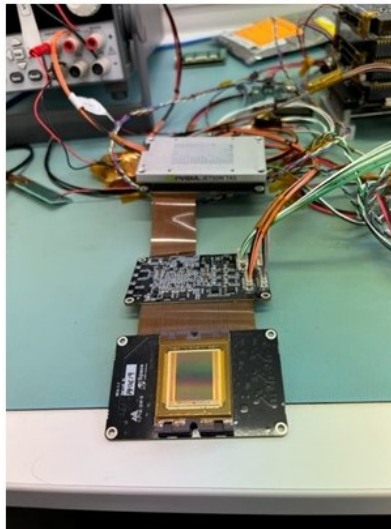


Figure 13. Edge Computing Module - Jetson GPU.

Fire and lightning images contain a complexity of data items that when transmitted to the ground can be analyzed to determine the basic science of fires and their ignition. However, small form factor platforms such as CubeSats have a very limited communications bandwidth and therefore lend themselves well to preconditioning or on-board processing of images. This requires at least a basic form of artificial intelligence or machine learning (ML) which can be accommodated using edge computing hardware and techniques.

The UNSW M2A & M2B spacecraft demonstrated that AI/ML algorithms applied through edge computing could improve image analysis of large field of views to classify objects, identify temporal change, and detect clouds for their removal from satellite or aerial imagery.³⁹ This can provide both a detection capability for smoke as it has some common optical panchromatic qualities to cloud and/or provide an image quality control aspect to discriminate images with cloud or smoke. In the case of M2A, M2B AI/ML algorithms were used to detect cloud and select cloud free images for transmission from the spacecraft to the Earth station. Using edge computing approach, M2A & M2B significantly reduced downlink bandwidth. Images from the UNSW M2 AB 80 mm telescopes were obtained from 534 km altitude and 45 degree inclination during the La Niña weather cycle in 2021-22. This produced many cloud effected images. Whilst this diminished ground imaging abilities, it offered an opportunity to experiment with the M2 artificial intelligence payload and software.

The M2 A&B spacecraft Image Processing Assembly (IPA) containing the 80 mm optical telescope incorporated an Field Programmable Gate Array (FPGA) and edge computing cards with embedded processing capabilities. It required the development of algorithms to identify feature extraction, the selection of AI-capable processing systems to interface between FPGA and edge computers that are survivable in Low Earth Orbit (LEO). Control logic in the FPGA and edge computer and a process for generating required imager datasets was required to train the processors to discriminate for cloud through an examination of techniques that rely on region-based classifiers (e.g., R-CNN, Fast R-CNN, and YOLO). Similar approaches could be utilized in case of images affected by smoke.

In the case of the M2 mission, a machine learning model implemented on a Jetson TX2 GPU card (Figure 13) and trained to identify clouds in images from a gray-scale database of images containing clouds. It was 75% successful when used on a small dataset 12 images.

The airborne phase of the mission will be used to test the same edge computing configuration and we propose similar hardware however the machine learning model can also be trained to detect bushfire features (e.g. smoke, thermal hotspots) and be trained from a much larger dataset.

5.4 Visible Imager

A visible imager to detect the direction of smoke completes the sensor suite. A commercially available imager from Dragonfly Aerospace is baselined as the visible imager. The Gecko imager (Figure 14) is an easy-to-integrate imaging solution designed for CubeSat missions.



Figure 14. Dragonfly Aerospace Gecko Visible Imager.

Large high speed data storage is integrated into the compact design. It provides color snapshot images and high frame rate video with 39 m resolution (at 500 km) and 80 km swath in 1U (10×10×10 cm) form factor. RGB images are captured at up to 5 frames per second using a matrix sensor in snapshot (global shutter) mode. Data may be streamed out to an on-board computer and down linked at a lower data rate, as required.

6. ORBITAL MISSION

In the orbital phase of this project, the payloads will be integrated into a CubeSat platform to be launched into a Sun Synchronous Orbit at an altitude of 500 kms. A local time of the ascending node (LTAN) of 16:30 hours will close the current deficiency in the observational window as needed by various Australian government agencies.

6.1 Spacecraft Specifications

The spacecraft selected for this mission is a 12U (30×20×20 cm) platform, shown in Figure 15, manufactured by Hex 20 Ltd, based in Adelaide, South Australia. Hex 20 heritage traces to missions associated with Laboratory for Atmospheric and Space Physics (LASP), University of Colorado. The platform is a high-performance, high

Technology Readiness Level (TRL) bus with state-of-the-art CubeSat pointing and data downlink capabilities. The spacecraft will accommodate the multiband thermal imager and the secondary payloads, although it should be noted that 12U is baseline size pending detailed mission profile studies.

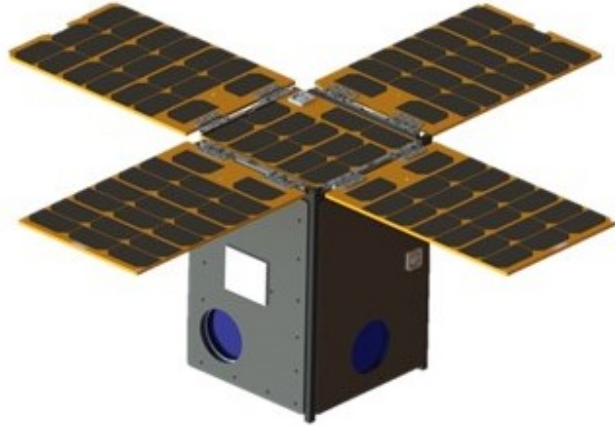


Figure 15. A rendering of the 12U CubeSat baselined for the orbital mission is given above.

The thermal imager will be installed nadir pointing to image the ground during each orbit. A high-level spacecraft architecture, subsystems, and spacecraft overall performance specification is given in Table 2, and detailed specifications are given elsewhere.⁴⁰ The spacecraft leverages heritage components compliant with most commercially available CubeSat deployers.

The spacecraft has four deployable panel arrays and one fixed panel providing 100 Watts of system power at the end of life (110 W at the beginning of life). Two 99 Wh batteries have a nominal depth of discharge for each orbit when accommodating 10 minutes of science downlink per orbit, spacecraft beaconing throughout the entire orbit, and 10 minutes of UHF command and control. All the spacecraft components have proven flight heritage. The spacecraft subsystems are rated at Technology Readiness Level (TRL) of 9 and the respective missions are given in Table 3.

Table 2. Spacecraft Specifications

Parameter	30 × 20 × 20 (12U)
Mass	20 kg
Power	110 W (Peak), 67 W (Average), 198 WH battery (2 Packs)
Communications	UHF (9600 bps), X-Band (15 mbps)
Interfaces	IC, UART, RS 232, RS 422, SPI
Voltage Lines	8.4 V (Battery), 12V, 6V, 3.3V
Pointing Accuracy	±0.003 ° (12") in 2 axis ±0.007 ° (26") in 3 rd axis

6.1.1 Ground Segment

The Hex20 satellite operations center is connected to ground stations in Adelaide (South Australia), Perth (Western Australia), Boulder CO and NTU Singapore for X-band. All have full UHF capability for spacecraft command and control, and low-rate science downlink (9.6 kbps, 19.2 kbps). All UHF stations are licensed in the amateur band at 437 MHz for uplink and downlink and the Singapore station is also licensed for X-band downlink at 8.320 GHz.

Table 3. Spacecraft Mission Heritage

Component	Mission Heritage
On Board Processor	INSPIRESAT-1, IDEASAT
Electrical Power Distribution	MinXSS,INSPIRESAT-1, IDEASAT, INSPIRESat-4
Battery Pack	VELOX II, Aoba-VELOX, INSPIRESat-4, VELOX AM
Solar Panels	CSSWE, MinXSS, INSPIRESAT-1
BCT XCAT ADCS	MinXSS, IS-1, Raven, RainCube, Marco
SpaceQuest TRX-U UHF Transceiver	IS-1, CSIM, IS-4, SCOOB-II, Multiple Microsat missions
Syrlinks EWC27 X-Band Transmitter	CSSWEE, MinXSS, IS-1, SCOOB-1
Antenna Deployment Module	CNES/ESA Rosetta, Proba-V
Thrustme NPT-30 12 Thruster	Chinese Mission: Satellite Catalogue number 46838, IS-4

The ground station in Singapore is owned by the Satellite Research Centre (SaRC) at NTU Singapore. This has a 6.1- meter dish with S-band uplink and downlink and X-band downlink capability. The infrastructure and hardware are expected to be in place to support ground system testing and flight operations.

Software tools with extensive flight heritage are in place and are customized for each mission to support real-time commanding and telemetry monitoring, alert notification, planning and scheduling operations, data trending and analysis, and science data processing. NTU will downlink and pipe the data to a cloud server which will be archived by Hex20 data systems. Before launch, the satellites will undergo a ground compatibility test with the ground stations. UNSW Canberra and Edith Cowan University also have mission control and ground stations to support this mission. UNSW Canberra has state of the art facilities that were used for their M2M and Buccaneer missions. UNSW Canberra Space is equipped with two satellite ground stations, one located on campus, while a larger industrial-grade satellite is positioned just outside the Australian Capital Territory (ACT) border in Yass. The Yass ground station is the primary operational facility for in-orbit communication and operation of satellites, while the on-campus ground station is used for satellite communications research and as a backup for Yass.

A University of Adelaide mission control and ground station at its Roseworthy campus will become operational by 2025, adding another layer of capability. All these facilities will be augmented by University of Tasmania’s spacecraft tracking facility which has 6 antennas, including a 26 meter dish. This facility supports operation in L-band, S-band, C-band and, X-band, K-band.

These facilities will provide the extra redundancy needed for a mission of this nature and it will help to mitigate any risk at an operational facility to enable seamless operation for control and down linking data which will be uploaded onto a secure cloud server for access by multiple users.

ACKNOWLEDGMENTS

The assistance provided by Dr. Robert Warren from Bureau of Meteorology, Australia, Ms. Julie Breed at NASA GSFC and Mr. Neil Martin at NASA MSFC is warmly appreciated. The authors wish to acknowledge the Sir Ross and Sir Keith Smith Fund for their continued support for this work. Edith Cowan University financial support for conference is gratefully acknowledged.

REFERENCES

- [1] Cresswell, I., Janke, T. and Johnston, E.L., “Biodiversity — Australia State of the Environment 2021,” report, Department of Agriculture, Water and the Environment, The Commonwealth of Australia (July 2022).

- [2] Binskin, M., Bennett, A., and Macintosh, A., “Royal Commission into National Natural Disaster Arrangements - Final Report,” (Oct 2020).
- [3] Wen, B., Wu, Y., Xu, R., Guo, Y., and Li, S., “Excess emergency department visits for cardiovascular and respiratory diseases during the 2019–20 bushfire period in Australia: A two-stage interrupted time-series analysis,” *Science of the Total Environment* **809** (Feb. 2022).
- [4] Fasullo, J., Rosenbloom, N., and Buchholz, R., “A multiyear tropical Pacific cooling response to recent Australian wildfires in CESM2,” *Science Advances* **9**, eadg1213 (May 2023).
- [5] Canadell, J. G., Meyer, C. P., Cook, G. D., Dowdy, A., Briggs, P. R., Knauer, J., Pepler, A., and Haverd, V., “Multi-decadal increase of forest burned area in Australia is linked to climate change,” *Nature Communications* **12**, 6921 (2021).
- [6] Abram, N. J., Henley, B. J., Sen Gupta, A., Lippmann, T. J. R., Clarke, H., Dowdy, A. J., Sharples, J. J., Nolan, R. H., Zhang, T., Wooster, M. J., Wurtzel, J. B., Meissner, K. J., Pitman, A. J., Ukkola, A. M., Murphy, B. P., Tapper, N. J., and Boer, M. M., “Connections of climate change and variability to large and extreme forest fires in southeast Australia,” *Communications Earth & Environment* **2**, 8 (Jan. 2021).
- [7] Bowman, D. M. and Sharples, J. J., “Taming the flame, from local to global extreme wildfires,” *Science* **381**, 616 – 619 (2023).
- [8] Sharples, J. J., Cary, G. J., Fox-Hughes, P., Mooney, S., Evans, J. P., Fletcher, M.-S., Fromm, M., Grierson, P. F., McRae, R., and Baker, P., “Natural hazards in Australia: extreme bushfire,” *Climatic Change* **139**, 85–99 (November 2016).
- [9] Di Virgilio, G., Evans, J. P., Blake, S. A. P., Armstrong, M., Dowdy, A. J., Sharples, J., and McRae, R., “Climate Change Increases the Potential for Extreme Wildfires,” *Geophysical Research Letters* **46**(14), 8517–8526 (2019).
- [10] McRae, R., “Australian PyroCb Register.” <https://www.highfirerisk.com.au/pyrocb/register.htm> (2024). Accessed 29 July 2024.
- [11] Peterson, D. A., Fromm, M. D., Solbrig, J. E., Hyer, E. J., Surratt, M. L., and Campbell, J. R., “Detection and Inventory of Intense Pyroconvection in Western North America using GOES-15 Daytime Infrared Data,” *Journal of Applied Meteorology and Climatology* **56**(2), 471 – 493 (2017).
- [12] Peterson, D. A., Fromm, M., McRae, R., Campbell, J., Hyer, E., Taha, G., Camacho, C., Kablick, G., Schmidt, C., and DeLand, M., “Australia’s Black Summer pyrocumulonimbus super outbreak reveals potential for increasingly extreme stratospheric smoke events,” *npj Climate and Atmospheric Science* **4**(38) (2021).
- [13] Sharples, J. J., Hilton, J. E., Badlan, R. L., Thomas, C. M., and McRae, R. H. D., [*Fire Line Geometry and Pyroconvective Dynamics*], 77–128, Cambridge University Press (2022).
- [14] Cai, D., Abram, N., Sharples, J., and Perkins-Kirkpatrick, S., “Increasing intensity and frequency of cold fronts contributed to Australia’s 2019-2020 Black Summer fire disaster,”
- [15] Jenkins, M., Holmes, A., Monks, J., Runcie, J., Sauvage, S., and Matthews, S., “The Australian Fire Danger rating System Ignition, Suppression and Impact Indices,” tech. rep., NSW Rural Fire Service (2022).
- [16] Holle, R., “Some Aspects of Global Lightning Impacts,” *2014 International Conference on Lightning Protection, ICLP 2014* (Oct 2014).
- [17] Fuquay, D. M., Taylor, A. R., Hawe, R. G., and Schmid Jr., C. W., “Lightning discharges that caused forest fires,” *Journal of Geophysical Research (1896-1977)* **77**(12), 2156–2158 (1972).
- [18] Pérez-Invernón, F. J., Moris, J. V., Gordillo-Vázquez, F. J., Füllekrug, M., Pezzatti, G. B., Conedera, M., Lapierre, J., and Huntrieser, H., “On the Role of Continuing Currents in Lightning-Induced Fire Ignition,” *Journal of Geophysical Research: Atmospheres* **128**(21), e2023JD038891.
- [19] Schultz, C., Bitzer, P., Antia, M., Case, J., and Hain, C., “Assessing Flash Characteristics in Lightning-Initiated Wildfire Events between 1995 and 2020 within the Contiguous United States,” *Journal of Applied Meteorology and Climatology* **63** (April 2024).
- [20] Krause, A., Kloster, S., Wilkenskjeld, S., and Paeth, H., “The sensitivity of global wildfires to simulated past, present, and future lightning frequency,” *Journal of Geophysical Research: Biogeosciences* **119**(3), 312–322 (2014).

- [21] Pérez-Invernón, F. J., Gordillo-Vázquez, F., Huntrieser, H., and Jöckel, P., “Variation of lightning-ignited wildfire patterns under climate change,” *Nature Communications* **14**, 739 (Feb 2023).
- [22] Dowdy, A. and Ga, M., “Characteristics of lightning-attributed fires in South-East Australia,” *International Journal of Wildland Fire* **21**, 521–524 (Jan 2012).
- [23] Owens, D. and O’Kane, M., “NSW Bushfire Inquiry report,” (July 2020).
- [24] Weatherzone Business, “Total lightning network.” <https://business.weatherzone.com.au/solution/total-lightning-network/> (2024). Accessed 29 July 2024.
- [25] Thomas, R. J., Krehbiel, P. R., Rison, W., Hunyady, S. J., Winn, W. P., Hamlin, T., and Harlin, J., “Accuracy of the Lightning Mapping Array,” *Journal of Geophysical Research: Atmospheres* **109**(D14) (2004).
- [26] Medina, B. L., Carey, L. D., Lang, T. J., Bitzer, P. M., Deierling, W., and Zhu, Y., “Characterizing Charge Structure in Central Argentina Thunderstorms During RELAMPAGO Utilizing a New Charge Layer Polarity Identification Method,” *Earth and Space Science* **8**(8), e2021EA001803.
- [27] Fairman, S. I. and Bitzer, P. M., “The Detection of Continuing Current in Lightning Using the Geostationary Lightning Mapper,” *Journal of Geophysical Research: Atmospheres* **127**(5), e2020JD033451.
- [28] Goodman, S. J., Blakeslee, R. J., Koshak, W. J., Mach, D., Bailey, J., Buechler, D., Carey, L., Schultz, C., Bateman, M., McCaul, E., and Stano, G., “The GOES-R Geostationary Lightning Mapper (GLM),” *Atmospheric Research* **125-126**, 34–49 (2013).
- [29] eoPortal: Satellite Missions Catalogue, “MTG (Meteosat Third Generation).” <https://www.eoportal.org/satellite-missions/meteosat-third-generation/eop-quick-facts-section> (2023). Accessed 29 July 2024.
- [30] Cao, D., Lu, F., Zhang, X., and Yang, J., “Lightning Activity Observed by the FengYun-4A Lightning Mapping Imager,” *Remote Sensing* **13**(15) (2021).
- [31] Lang, T. J., Ávila, E. E., Blakeslee, R. J., Burchfield, J., Wingo, M., Bitzer, P. M., Carey, L. D., Deierling, W., Goodman, S. J., Medina, B. L., Melo, G., and Pereyra, R. G., “The relampago lightning mapping array: Overview and initial comparison with the geostationary lightning mapper,” *Journal of Atmospheric and Oceanic Technology* **37**(8) (2020).
- [32] Zhu, Y., Bitzer, P., Stewart, M., Podgorny, S., Corredor, D., Burchfield, J., Carey, L., Medina, B., and Stock, M., “Huntsville Alabama Marx Meter Array 2: Upgrade and Capability,” *Earth and Space Science* **7**(4), e2020EA001111.
- [33] Gatlin, P. et al, “Cubespark: A New Satellite-Based 3d Lightning Observing Concept,” report, NASA Marshall Space Flight Center (January 2022).
- [34] Quick, M., Gatlin, P., Bitzer, P., Lang, T., and Ostgaard, N., “Multi-band lightning optical emission from tropical storms recorded during the Airborne Lightning Observatory for Fly’s Eye GLM Simulator and Terrestrial Gamma-Ray Flashes Flight Campaign,” in [*Earth Observing Systems XXVIII*], Xiong, X. J., Gu, X., and Czaplá-Myers, J. S., eds., **12685**, 1268506, International Society for Optics and Photonics, SPIE (2023).
- [35] Jhabvala, M. D., Jennings, D. E., Tucker, C., La, A. T., Keer, B., Timmons, E., Stone, R., Flatley, T. W., Cepollina, F., Babu, S. R., Lunsford, A. W., Cassidy, J. C., Parker, D., Sundaram, M., Bundas, J., Squicciarini, W., Finneran, P., Orłowski, I., Fetter, C., and Loose, M., “Strained-layer-superlattice-based compact thermal imager for the International Space Station,” *Applied Optics* **58**, 5432–5442 (2019).
- [36] Choi, K.-K., Jhabvala, M., Jennings, D., Turck, K., La, A., Wu, D., Hewagama, T., Holmes, T., Flatley, T., Cillis, A., Fitts, Y., and Morton, D., “Remote temperature sensing by the compact thermal imager from the International Space Station,” *Appl. Opt.* **60**, 10390–10401 (Nov 2021).
- [37] Christian, H. J. et al, “The lightning imaging sensor,” report, NASA Marshall Space Flight Center (June 1999).
- [38] Quick, M., Christian, H., Virts, K., and Blakeslee, R., “Airborne radiometric validation of the geostationary lightning mapper using the fly’s eye glm simulator,” *Journal of Applied Remote Sensing* **14** (Oct 2020).
- [39] Harrison, R., “RAAF & UNSW Canberra M2 CubeSats Successfully separate in Orbit.” <https://spaceaustralia.com/news/raaf-uns-w-canberra-m2-cubesats-successfully-separate-orbit> (September 2021). Accessed 29 July 2024.
- [40] Hex20 Pty Ltd, “Product satellite platform.” <https://hex20.com.au/> (2024). Accessed 29 July 2024.